



June 2007

Effects of Ta addition on the microstructure and mechanical properties of $Ti_{40}Zr_{25}Ni_8Cu_9Be_{18}$ amorphous alloy

Jinna Mei

State Key Laboratory of Solidification Processing, Northwestern Polytechnical University, Xi'an 710072, China

Jinshan Li

State Key Laboratory of Solidification Processing, Northwestern Polytechnical University, Xi'an 710072, China

Hongchao Kou

State Key Laboratory of Solidification Processing, Northwestern Polytechnical University, Xi'an 710072, China

Rui Hu

State Key Laboratory of Solidification Processing, Northwestern Polytechnical University, Xi'an 710072, China

Hengzhi Fu

State Key Laboratory of Solidification Processing, Northwestern Polytechnical University, Xi'an 710072, China

See next page for additional authors

Follow this and additional Works at: <https://ustb.researchcommons.org/ijmmm>

Recommended Citation

Mei Jinna, Li Jinshan, Kou Hongchao, Hu Rui, Fu Hengzhi, Zhou Lian. Effects of Ta addition on the microstructure and mechanical properties of $Ti_{40}Zr_{25}Ni_8Cu_9Be_{18}$ amorphous alloy, *Int. J. Miner. Metall. Mater.*, 14 (2007), No. 7, Article 6, p. 31-35.

This Research is brought to you for free and open access by International Journal of Minerals, Metallurgy and Materials. It has been accepted for inclusion in International Journal of Minerals, Metallurgy and Materials by an authorized editor of International Journal of Minerals, Metallurgy and Materials.

Effects of Ta addition on the microstructure and mechanical properties of $\text{Ti}_{40}\text{Zr}_{25}\text{Ni}_8\text{Cu}_9\text{Be}_{18}$ amorphous alloy

Authors

Jinna Mei, Jinshan Li, Hongchao Kou, Rui Hu, Hengzhi Fu, and Lian Zhou

Effects of Ta addition on the microstructure and mechanical properties of $\text{Ti}_{40}\text{Zr}_{25}\text{Ni}_8\text{Cu}_9\text{Be}_{18}$ amorphous alloy

Jinna Mei¹⁾, Jinshan Li¹⁾, Hongchao Kou¹⁾, Rui Hu¹⁾, Hengzhi Fu¹⁾, and Lian Zhou^{1,2)}

1) State Key Laboratory of Solidification Processing, Northwestern Polytechnical University, Xi'an 710072, China

2) Northwest Institute for Nonferrous Metal Research, Xi'an 710016, China

(Received 2006-06-22)

Abstract: The effects of Ta addition on the microstructure and mechanical properties of $\text{Ti}_{40}\text{Zr}_{25}\text{Ni}_8\text{Cu}_9\text{Be}_{18}$ bulk amorphous alloy were investigated by using X-ray diffraction (XRD), transmission electron microscopy (TEM), scan electron microscopy (SEM) and compressive testing. As a result, the addition of Ta (0-8at%) prompted the successive precipitation of quasicrystalline phase, CuTi_2 phase and bcc β -Ti solid solution. Additionally, the addition of less Ta content (3at%-5at%) led to the formation of amorphous matrix/nanoquasicrystal/ CuTi_2 complex phase structure; and nanoquasicrystals, as reinforcement precipitates, improved the fracture strength of Ti-Zr-Ni-Cu-Be-Ta alloys, which led to the high compressive fracture strength 1856 MPa of Ta5 alloy. With increasing Ta content (5at%-8at%), although the ductile dendritic β -Ti solid solution was precipitated, the strength and plasticity decreased to a great extent resulting from the growth of quasicrystalline phase and CuTi_2 phase.

Key words: Ti-based amorphous alloy; bulk amorphous alloy; microstructure; mechanical properties

[This work was financially supported by the New Century Excellent Person Supporting Project, Science and Technology Foundation of Shaanxi Province of China, DPOP and Young Science and Technology Foundation in NWPU.]

1. Introduction

Bulk amorphous alloys are of scientific interest in material science field due to their unique mechanical, physical and chemical properties associated with the long-range disorder and short-range order atomic structure. Ti-based bulk amorphous alloys have lower density and higher specific strength [1-7], which are attractive for using as structural material in many fields. However, bulk amorphous alloys usually show very small plasticity due to the formation of highly localized shear bands under loading. Many attempts have been devoted to toughen the bulk amorphous alloys. In particular, the in-situ formed ductile dendritic (spherical) crystalline phases can significantly improve the plasticity of bulk amorphous alloys, which has been successfully shown in Zr-, La-, Pd-based bulk amorphous alloys [8-13]. Recently, G. He *et al.* have reported that the refractory element like Nb, Ta, Mo, *etc.* can prompt the precipitation of ductile crystalline phases in Ti-Ni-Cu-Sn and Ti-Ni-Cu-Sn-Zr amorphous alloys, which can lead to the enhancement of plasticity [8-9, 12-19].

Based on the analysis above,

$(\text{Ti}_{0.4}\text{Zr}_{0.25}\text{Ni}_{0.08}\text{Cu}_{0.09}\text{Be}_{0.18})_{100-x}\text{Ta}_x$ ($x=0, 3, 5, 8$) glassy alloys were prepared, and the effects of Ta addition on the microstructure and mechanical properties of $\text{Ti}_{40}\text{Zr}_{25}\text{Ni}_8\text{Cu}_9\text{Be}_{18}$ bulk amorphous alloy were researched in this work in detail.

2. Experimental

Master alloys with nominal compositions of $(\text{Ti}_{0.4}\text{Zr}_{0.25}\text{Ni}_{0.08}\text{Cu}_{0.09}\text{Be}_{0.18})_{100-x}\text{Ta}_x$ ($x=0, 3, 5, 8$) were prepared by arc melting mixtures of high purity metals (whose purities are above 99.5%) in a Ti-gettered argon atmosphere. In this experiment, for the melting point of Ta was up to 3293 K, the procedure of master alloy smelting was separated into two steps to ensure that the alloy composition was homogeneous. Firstly, melting Ta-Zr intermediate alloy 2-3 times to decrease the alloy melting point; secondly, putting other metals into Ta-Zr intermediate alloy and then melting 3-4 times till the master alloy was homogeneous; finally, the bulk alloys in a cylindrical form with a diameter of 3 mm were prepared by the suction casting method. The samples were then cut into $\phi 3 \text{ mm} \times 2 \text{ mm}$ and $\phi 3 \text{ mm} \times 6 \text{ mm}$ specimens on the linear cutting machine

for the following analysis and testing. The phase structure of specimens was identified by XRD (PHILIPS X'Pert Pro, monochromatic Cu K_{α} radiation), SEM (JEOLJSM-5610LV equipped with X-ray energy-dispersive spectrometry (EDS)) and TEM (JEM-200CX, JEM-3010 equipped with selected-area electron diffraction pattern (SADP)). Thinning of the specimens for TEM measurement was prepared by mechanically grinding to a 60 μm -thick plate firstly and then twin-jet electrolytic thinning using a solution mixed in the ratio of $\text{HClO}_4:\text{CH}_3\text{OH}=5\%:95\%$. Uniaxial compression tests were conducted on the ZMT5305-type machine under the constant cross-head speed condition of an initial strain rate of 10^{-4} s^{-1} at room temperature. The samples were deformed until fracture occurred, and then the fracture surface of the failed samples was observed by SEM (JEOLJSM-5610LV).

3. Results and discussion

3.1. Microstructure analysis

Fig. 1 shows the XRD patterns of as-cast $(\text{Ti}_{0.4}\text{Zr}_{0.25}\text{Ni}_{0.08}\text{Cu}_{0.09}\text{Be}_{0.18})_{100-x}\text{Ta}_x$ ($x=0, 3, 5, 8$) bulk alloys (abbr. Ta0, Ta3, Ta5 and Ta8 alloy). Broad halo feature reveals the glassy state of Ta0 alloy. However, there exists an appreciable diffraction peak in the XRD pattern of Ta3 alloy, which demonstrates that a few crystals form in the amorphous matrix. Obviously, with increasing the Ta content from 3at% to 8at%, quasicrystalline phase, CuTi_2 phase and bcc β -Ti solid solution were precipitated successively.

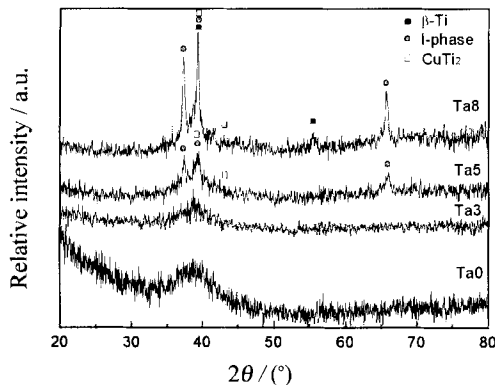


Fig. 1. XRD patterns obtained from $(\text{Ti}_{0.4}\text{Zr}_{0.25}\text{Ni}_{0.08}\text{Cu}_{0.09}\text{Be}_{0.18})_{100-x}\text{Ta}_x$ ($x=0, 3, 5,$ and 8) alloys.

Figs. 2(a)-(c) show the microstructures of as-cast Ta3, Ta5 and Ta8 bulk alloys, respectively. The TEM image of Ta3 alloy shows that no crystal is precipitated in the amorphous matrix, and the diffuse halo pattern of SADP reveals the glassy state of the bulk specimen. However, according to the XRD pattern, there do exist a few crystals. The reason why no crys-

tal can be observed in the TEM image of Ta3 alloy is that the precipitations are very little and distributed nonhomogeneously in the amorphous matrix. While Fig. 2(b) shows that in Ta5 alloy, some crystals with the size of 10-40 nm are homogeneously distributed in the amorphous matrix. Additionally, a few rodlike crystals form in the amorphous matrix. By using XRD, TEM and corresponding SADP, the precipitated phases are analyzed to be icosahedral quasicrystalline phase (I phase) and CuTi_2 phase ($a=0.2943 \text{ nm}$, $c=1.078 \text{ nm}$). When the Ta content is up to 8at%, there only exists a little remaining amorphous structure. Further observation reveals that a few dendrites with large scale of grain size are embedded in the amorphous matrix besides large quantity of quasicrystals. Fig. 3 just shows the detailed amorphous matrix/quasicrystal/dendrite complex phase structure in Ta8 alloy. The average secondary dendritic arm space λ_2 of dendrites is measured to be about 400 nm. Combining the SADP and EDS analysis, the dendrites are demonstrated to be Ta-rich bcc β -Ti solid solution whose crystal lattice constant is calculated to be $a=0.3365 \text{ nm}$. In Fig. 3(b) the zone axis of SADP is $[001]$. In addition, a few rodlike crystals are also distributed in the matrix. Fig. 4 just shows the TEM image of the rodlike crystals, which are dendrites actually; nevertheless the growth of the secondary dendritic arm is restricted.

The EDS results, which were obtained from the icosahedral quasicrystalline phase and dendrite (β -Ti solid solution) in Ta8 alloy, reveal that the chemical composition of these two crystalline phases is significantly different. In detail, the Ta element content in dendrites is about twice of that in quasicrystals, which indicates that the addition of high melting point element Ta can prompt the precipitation of bcc β -Ti solid solution and the enrichment in Ta, as is accordance with the reports of G. He *et al.* [14-17, 19]. Additionally, the effect of Ta is similar with that of Nb on the Ti-Zr-Ni-Cu-Be alloy system [20], since the Ti-Zr-Ni ternary alloy system is a typical quasicrystalline alloy system, the addition of Ta destroys the microstructure of the initial alloy, which leads to the nucleation and growth of I phase, CuTi_2 phase and bcc β -Ti solid solution.

3.2. Mechanical properties

Fig. 5 shows the compressive stress-strain curves at room temperature of Ta0, Ta3, Ta5 and Ta8 alloys, which indicates that the compressive fracture strength exhibits the trend of increasing firstly and then decreasing with increasing the Ta content, while the plastic strain decreases rapidly till absolute no plastic-

ity.

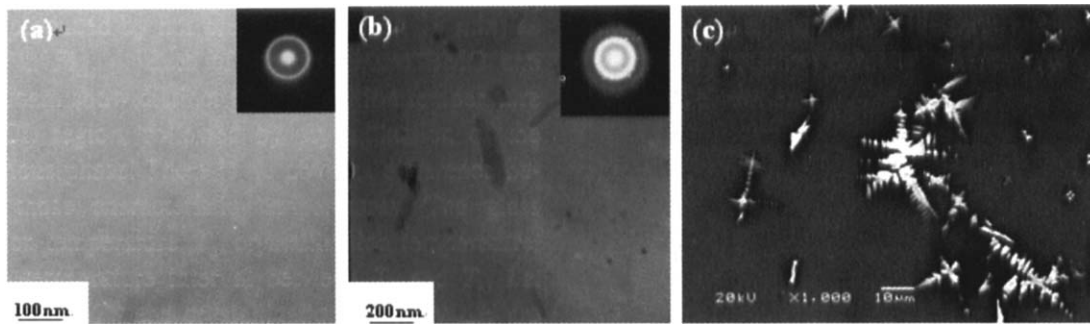


Fig. 2. Microstructure of as-cast $(\text{Ti}_{0.4}\text{Zr}_{0.25}\text{Ni}_{0.08}\text{Cu}_{0.09}\text{Be}_{0.18})_{100-x}\text{Ta}_x$ ($x=3, 5, 8$) alloys: TEM images of Ta3 (a) and Ta5 (b); SEM image of Ta8 (c).

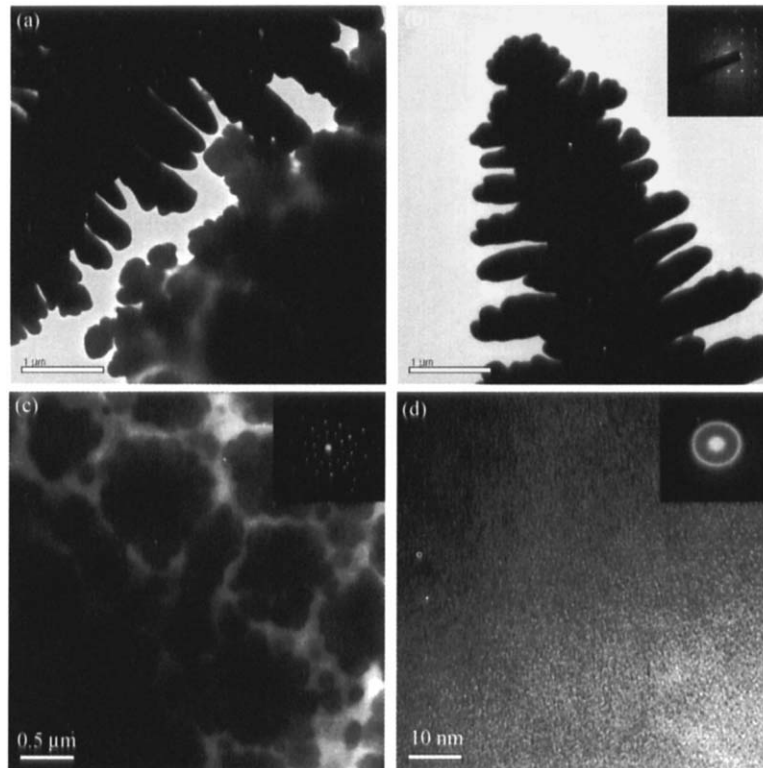


Fig. 3. Typical bright field image obtained from amorphous/quasicrystalline/dendritic structure in Ta8 alloy (a), dendrite (b), quasicrystal (c), and amorphous matrix (d).

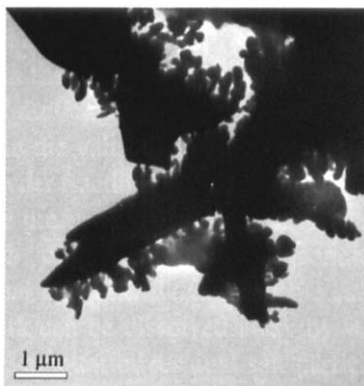


Fig. 4. Typical bright field image obtained from CuTi_2 phase in Ta8 alloy.

Fig. 6 shows the micrographs of the fracture surface of failed Ta0, Ta3, Ta5 and Ta8 alloys. The well-developed vein patterns can be observed on the fracture surface of Ta0 and Ta3 alloys, which reveals that

their fracture modes are both ductile fractures. However, the fracture surface of Ta5 alloy consists of smooth and vein pattern regions. The smooth region

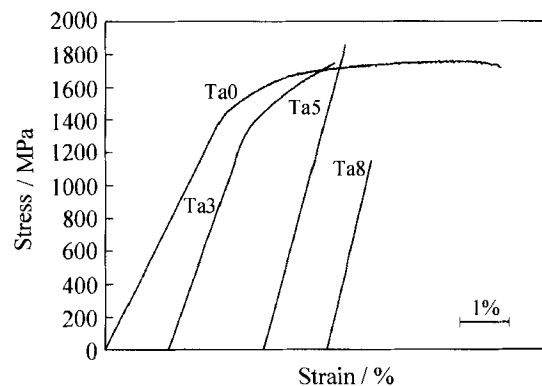


Fig. 5. Compressive stress-strain curves at room temperature for $(\text{Ti}_{0.4}\text{Zr}_{0.25}\text{Ni}_{0.08}\text{Cu}_{0.09}\text{Be}_{0.18})_{100-x}\text{Ta}_x$ ($x=0, 3, 5, 8$) alloys.

results from shear sliding, and the distinctly developed shear bands on the fracture surface shows that the local shear deformation enhances the degree of local adiabatic heating at the final fracture stage, leading to a significant viscous flow of the glassy matrix. In addition, the shear bands for the Ta5 alloy are almost parallel to the shear stress direction indicating rapid

crack propagation, resulting in a brittle fracture [21]. When the Ta content is up to 8at%, the fracture surface which exhibits the characteristic of shallow corrugated liquid flow is significantly different from that of the above three alloys, as demonstrates that Ta8 alloy appears melting phenomenon widely during the compressive deformation.

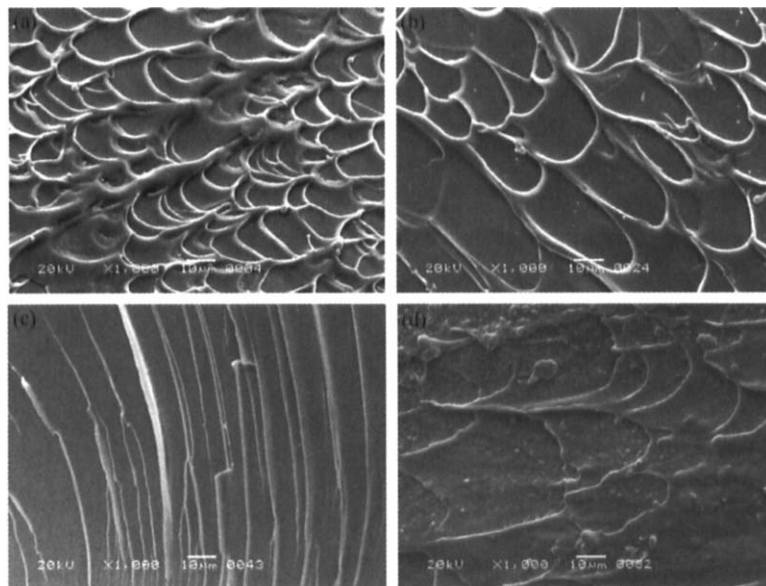


Fig. 6. SEMs of the fracture surface of the failed $(\text{Ti}_{0.4}\text{Zr}_{0.25}\text{Ni}_{0.08}\text{Cu}_{0.09}\text{Be}_{0.18})_{100-x}\text{Ta}_x$ ($x=0, 3, 5, 8$) alloys: (a) Ta0; (b) Ta3; (c) Ta5; (d) Ta8.

Comparing Ta0 alloy with Ta3 alloy, the compressive fracture strength of these two alloys is almost equivalent, while the plastic strain decreases from 4.4% (Ta0) to 1.1% (Ta3) resulting from the precipitation of less nanoquasicrystals in Ta3 alloy.

Ta5 alloy exhibits relative better compressive fracture strength of up to 1856 MPa. The addition of less Ta content ($\leq 5\text{at}\%$) can prompt the precipitation of less nanosized quasicrystals in the amorphous matrix. Thus the alloy can be strengthened. However, the precipitation of quasicrystals and CuTi_2 brittle phase leads to the final brittle fracture.

With increasing Ta content ($>5\text{at}\%$), the quasicrystals nucleate and grow up continuously, so the quasicrystals cannot play the role of reinforcement phase anymore; as a result, the strength of the alloy decreases significantly. On the other hand, the grain size of quasicrystals reaches micron dimension, and CuTi_2 is a brittle phase, the plasticity still decreases till the plastic strain reaches 0, although the ductile dendritic bcc β -Ti solid solutions are precipitated in the matrix. This result is different from that of G. He *et al.*, who reported that the as cast Ti-Ni-Cu-Sn and Ti-Ni-Cu-Sn-Zr system alloy containing Ta element exhibited relatively good plasticity and strength at room temperature due to the impediment of plastic dendrites to

shear bands of the amorphous matrix and their initial plastic deformation [8, 14-16, 18]. As we know the properties of the composite depend on the properties of its matrix and secondary phase, while the microstructure, distribution, volume fraction, size *etc.* of the secondary phase significantly affect the performance of the composite as well as the amorphous matrix composite. Moreover, the properties of bulk amorphous alloys are very sensitive to brittle phase. Thus, comparing with the results of G. He, in our experiment, the addition of Ta is put into neither Ti-Ni-Cu-Sn nor Ti-Ni-Cu-Sn-Zr system but Ti-Zr-Ni-Cu-Be system, which leads to the precipitation of different crystalline phases. Besides bcc β -Ti solid solutions, quasicrystalline and CuTi_2 brittle phases are both embedded, and the distributions of precipitated phases are not so homogeneous as G. He's results, as leads to the rapid decreasing of plasticity. In summary, the composite consisting of dendrites (equiaxed crystal or spherical crystal) embedded in the homogeneous matrix in which there exists no other brittle precipitated phases can exhibit good plasticity.

4. Conclusions

(1) With increasing the Ta content from 0 to 8at%, the microstructure evolution of as-cast Ti-Zr-Ni-Cu-Be-Ta alloy is as the following: amorphous (Ta0)→

amorphous + quasicrystal (Ta3) → amorphous + quasicrystal + CuTi₂ (Ta5) → amorphous + quasicrystal + CuTi₂ + dendritic β-Ti (Ta8).

(2) The addition of Ta (0-8at%) prompts the precipitation of quasicrystalline phase, CuTi₂ phase and bcc β-Ti solid solution.

(3) The addition of less Ta content (3at%-5at%) leads to the formation of amorphous matrix/nanocrystal/CuTi₂ complex phase structure. And nanocrystals, as reinforcement precipitates, make the fracture strength of Ti-Zr-Ni-Cu-Be-Ta alloys improved. When the Ta content is 5at%, the compressive fracture strength is up to 1856 MPa. With the further increasing of Ta content (5at%-8at%), although the ductile dendritic β-Ti solid solution is precipitated, the strength and plasticity decrease to a great extent resulting from the growth of quasicrystalline phase and CuTi₂ phase.

References

- [1] C.L. Ma, N. Nishiyama, and A. Inoue, Fabrication and characterization of Coriolis mass flowmeter made from Ti-based glassy tubes, *Mater. Sci. Eng. A*, 407(2005), No.1-2, p.201.
- [2] W.L. Johnson, Bulk glass-forming metallic alloys, *MRS Bull.*, 24(1999), No.10, p.42.
- [3] T. Zhang and A. Inoue, Mechanical properties of Zr-Ti-Al-Ni-Cu bulk amorphous alloy prepared by squeeze casting, *Mater. Trans. JIM*, 39(1998), No.12, p.1230.
- [4] A. Inoue and T. Zhang, Stabilization of supercooled liquid bulk glassy alloys in ferrous and non-ferrous system, *J. Non Cryst. Solids*, 250-252(1999), No.2, p.552.
- [5] A. Inoue, Stabilization of metallic supercooled liquid and bulk amorphous alloys, *Acta Mater.*, 48(2000), No.1, p.279.
- [6] D.V. Louzguine and A. Inoue, Nanocrystallization of Ti-Ni-Cu-Sn amorphous alloy, *Scripta Mater.*, 43(2000), No.44, p.371.
- [7] M.X. Xia, C.L. Ma, H.X. Zheng, et al., Preparation and crystallization of Ti₅₃Cu₂₇Ni₁₂Zr₃Al₇Si₃B₁ bulk metallic glass with wide supercooled liquid region, *Mater. Sci. Eng. A*, 390(2005), No.1-2, p.372.
- [8] G.Y. Sun, G. Chen, C.T. Liu, and G.L. Chen, Innovative processing and property improvement of metallic glass Based composites, *Scripta Mater.*, 55(2006), No.4, p.375.
- [9] C.C. Hays, C.P. Kim, and W.L. Johnson, Microstructure controlled shear band pattern formation and enhance plasticity of metallic glasses containing in situ formed ductile phase dendrite dispersions, *Phys. Rev. Lett.*, 84(2000), No.13, p.2901.
- [10] H. Tan, Y. Zhang, and Y. Li, Synthesis of La-based in-situ bulk metallic glass matrix composite, *Intermetallics*, 10(2002), No.11-12, p.1203.
- [11] X. Hu, S.C. Ng, Y.P. Feng, and Y. Li, Glass forming ability and in-situ composite formation in Pd-based bulk metallic glasses, *Acta Mater.*, 51(2003), No.2, p.561.
- [12] C. Fan, H.Q. Li, L.J. Kecskes, C.T. Liu, et al., Mechanical behavior of bulk amorphous alloys reinforced by ductile particles at cryogenic temperature, *Phys. Rev. Lett.*, 96(2006), p.145506.
- [13] Y.F. Sun, C.H. Shek, B.C. Wei, et al., Effect of Nb content on the microstructure and mechanical properties of Zr-Cu-Ni-Al-Nb glass forming alloys, *J. Alloy Compd.*, 403(2005), No.1-2, p.239.
- [14] G. He, J. Eckert, W. Löser, and L. Schultz, Novel Ti-based nanostructure-dendrite composite with enhanced plasticity, *Nat. Mater.*, 2(2003), No.1, p.33.
- [15] G. He, J. Eckert, W. Löser, et al., Composition dependence of the microstructure and the mechanical properties of nano/ultrafine-structured Ti-Cu-Ni-Sn-Nb alloys, *Acta Mater.*, 52(2004), No.10, p.3035.
- [16] G. He, W. Löser, and J. Eckert, Devitrification and phase transformation of (Ti_{0.5}Cu_{0.25}Ni_{0.15}Sn_{0.05}Zr_{0.05})_{100-x}Mo_x metallic glasses, *Scripta Mater.*, 50(2004), No.1, p.7.
- [17] G.J. Yang, T. Zhang, and A. Inoue, Effects of Ta, Nb and Mo additions on glass-forming ability of Ti₅₀Ni₂₀Cu₂₅Sn₅ amorphous alloy, *Rare Met. Mater. Eng.*, 32(2003), No.11, p.880.
- [18] C. Fan, R.T. Ott, and T.C. Hufnagel, Metallic glass matrix composite with precipitated ductile reinforcement, *Appl. Phys. Lett.*, 81(2002), No.6, p.1020.
- [19] G. He, J. Eckert, and M. Hagiwara, Mechanical properties and fracture behavior of the modified Ti-based bulk metallic glass-forming alloy, *Mater. Lett.*, 60(2006), No.5, p.656.
- [20] J.N. Mei, *Synthesis and Properties of Ti-Zr-Ni-Cu-Be Bulk Amorphous Alloy* [Dissertation] (in Chinese), Northwestern Polytechnical University, Xi'an, 2006, p.65.
- [21] G.Y. Yuan and A. Inoue, The effect of Ni substitution on the glass-forming ability and mechanical properties of Mg-Cu-Gd metallic glass alloys, *J. Alloy Compd.*, 387(2005), No.1-2, P.134.